JOURNAL OF SOLID STATE CHEMISTRY 95, 145–155 (1991)

Preparation and Characterization of Titanium Oxynitrides with High Specific Surface Areas

CHAE HO SHIN, GUY BUGLI, AND
GERALD DJEGA-MARIADASSOU*

Université P. et M. Curie, Laboratoire Réactivité de Surface et Structure, URA 1106 CNRS. 4, Place Jussieu, T54, 75252 Paris Cedex 05, France

Received December 26, 1990; in revised form June 25, 1991

Titania was reacted with ammonia between 890 and 1120 K to produce titanium oxynitride. The degree of nitridation and the specific surface area of the final solid products depend upon various factors such as gas composition, space velocity of the synthesis gas, heating rate, temperature and duration of isothermal treatment, and structure and texture of the starting material (commercial titania powder (P25, Degussa), titania aerogel or rhodium–titania aerogel). The influence of some of these parameters was investigated in the present study. Optimized operating conditions yielded specific surface areas ranging from 58 to 87 $m^2 g^{-1}$ depending on the starting material. The pore size distribution was centered on a 15–17 nm range. Titanium oxynitride crystallized in a face-centered cubic lattice. Above 70% nitridation, the X-ray diffraction data showed the presence of only one fcc phase; its lattice parameter increased with the nitrogen content, from a value close to that of fcc TiO, to a value approaching the parameter of fcc δ-TiN. Before exposure to air, samples had to be passivated in a flowing mixture of 1 vol% O_2 in He to prevent a rapid oxidation of the bulk.

1. Introduction

In the last years, transition-metal carbides and nitrides appeared to be promising compounds as catalysts for reactions traditionally catalyzed by noble metals (*1–5*) and more recently for hydrotreating processes (*6*). Oxynitrides and oxycarbides which can be either intermediates during the synthesis of nitrides and carbides (*7*) or the final products (*8*) may also be included in this field of research. However, to promote the catalytic activity of these materials, they must be prepared with high specific surface areas.

The simplest and most reliable method for preparing titanium oxynitrides consists in using a mixture of TiO and TiN in the required ratio as starting material. Thoroughly ground, this mixture is briquetted and sintered in vacuum at 1723 K (*9, 10*). Unfortunately, this classical route yields products with very low specific surface area.

The plasmochemical method has been used as an alternative method for preparation by Gurov *et al.* (*11*). Compounds have been synthetized by reducing $TiCl_4$ with hydrogen in a stream of nitrogen plasma containing small amounts of oxygen and water vapor. According to the operating conditions, oxynitrides with different N/O ratios could be obtained as powders with mean particle sizes ranging from 20 to 60 nm.

---

* To whom correspondence should be addressed.

0022-4596/91 $3.00

Another route involves titanium dioxide as starting material and ammonia as nitriding agent. It led to either oxynitrides (*12*) or nitride (*13, 14*) according to the temperature of reaction. In the former case, the method has been used to prepare sintered materials with a nitride surface layer; no detailed physicochemical characterization has been carried out.

Recent research (*7, 15, 16*) indicates that a temperature-programmed synthesis in a flowing ammonia stream using metal oxides as precursors can be a convenient method to prepare transition-metal nitrides with high surface areas.

The present study relates an attempt to extend this route for the synthesis of titanium oxynitrides. The effects of various operating conditions on the specific surface area and on the stoichiometry of the products were investigated.

2. Experimental

2.1. Materials

The gases employed in this study, without further purification, consisted of H_2 (Air Liquide, High Purity Grade, 99.995%), He (Air Liquide, High Purity Grade, 99.995%), NH_3 (Air Liquide, Custom Grade, 99.96%), and O_2 (Air Liquide, Custom Grade, 99.5%).

Different types of titanium dioxide were used as precursors for the synthesis of oxynitrides:

(i) Commercial titania powder (P25, Degussa) was a 1 : 1 anatase : rutile mixture with a surface area of 46 $m^2\ g^{-1}$. In order to render it more suitable for packing in the reactor, titania was wetted with distilled water (0.5 $cm^3\ g^{-1}$) and then dried in air at 423 K for 15 hr. This treatment did not affect the surface area of the dioxide.

(ii) Titania aerogel was prepared following the procedure described by Vicarini *et al.* (*17*).

(iii) Rhodium–titania aerogel was obtained according to the method developed by Teichner *et al.* (*18*), by hydrolysis of titanium tetrabutylate dissolved in 50 wt% butanol, with an appropriate aqueous solution of rhodium chloride. The solvent was then evacuated under hypercritical conditions in an autoclave.

In order to remove organic species adsorbed on their surface, these aerogels were treated at 573 K under flowing oxygen.

2.2. Elemental Analysis

The elemental composition of the products in nitrogen, oxygen, and titanium was measured at the Central Service of Chemical Analysis of the CNRS (Vernaison). The degree of nitridation was defined with respect to the theoretical content of nitrogen (22.6%) in stoichiometric titanium mononitride.

2.3. Powder X-Ray Diffraction

Structural characterization of the starting materials, intermediates, and oxynitrides was done by X-ray diffraction (XRD). Patterns were obtained with a Cu$K\alpha$ radiation on a Siemens Model D500 diffractometer. The lattice parameter of the face-centered cubic oxynitrides was determined using a refinement program (*19*). The average size of coherently diffracting domains perpendicular to (*hkl*) planes was evaluated by the Scherrer formula (*20*), from the half-width of the (*hkl*) X-ray line corrected for instrumental broadening.

2.4. Surface and Pore Size Measurements

Specific surface areas were determined by nitrogen adsorption at 77.4 K. The amounts of nitrogen adsorbed were measured in a conventional volumetric apparatus from pressure measurements with a capacitance manometer (type 590 Barocel Pressure Transducer with a 0–1000 Torr range). The nitrogen monolayer was estimated by the BET method (*21*) and the surface area was computed using a nitrogen cross section of 0.162 nm^2. The pore size distribution was obtained from an analysis of the desorption isotherm using the Barret, Joyner, and Halenda method (*22*).

2.5. *Electron Microscopy*

Electron microscopy was done using a JEOL JEM 100 CXII apparatus. Specimens for transmission electron microscopy (TEM) were dispersed ultrasonically in benzene and then deposited on a TEM copper grid coated with a holey carbon film.

2.6. *Synthesis Device*

Reactions with ammonia were carried out in a tubular quartz reactor provided with a coarse quartz fritted disk for holding the solid starting material. The reactor was heated by an electric furnace whose temperature was monitored with a programmable linear rate temperature controller (Setaram TGC 85). The gas mixtures (NH_3/He) were prepared by separate regulation of each gas stream with mass flow controllers (Brooks 5841-1). The gaseous products were analyzed by gas chromatography using a 2-m Porapak Q column at 323 K with an Intersmat IGC 12M thermal conductivity detector linked to a Hewlett–Packard 3390 A integrator.

2.7. *Synthesis Procedure*

During an experiment 0.2 to 0.5 g of titanium dioxide was nitrided at atmospheric pressure in a stream of ammonia and helium mixture with a volumetric ratio NH_3/He of 0.48 and a total flow rate ranging from 4 to 12 liters/hr. Different heating rates, temperatures, and durations of nitriding were used. After the nitriding treatment, the reactor was quickly cooled in the flowing reactant mixture and purged with helium at room temperature. Before exposure to air, each sample was passivated in a flowing mixture of 1 vol% O_2 in He to prevent a further possible rapid oxidation. After passivation the product batch was taken out and characterized.

3. Results

3.1. *Material Preparation*

A typical time evolution of ammonia decomposition during the temperature-programmed reaction of titanium dioxide with ammonia is shown in Fig. 1.

Titania began to react at about 843 K as evidenced by the decomposition of the reactant NH_3 and the darkening of the solid. At higher temperature, water vapor can also be detected in the chromatograms of the effluent gas but at a very low concentration. No precise endpoint of the synthesis was observed in this type of preparation.

The degree of nitridation and the specific surface area of the final solid products depend on various factors such as gas composition, space velocity of the synthesis gas (*16*), heating rate (*15*), temperature and duration of isothermal treatment, and structure (*7*) and texture of the starting material. The influence of some of these parameters was investigated in the present study. Re-

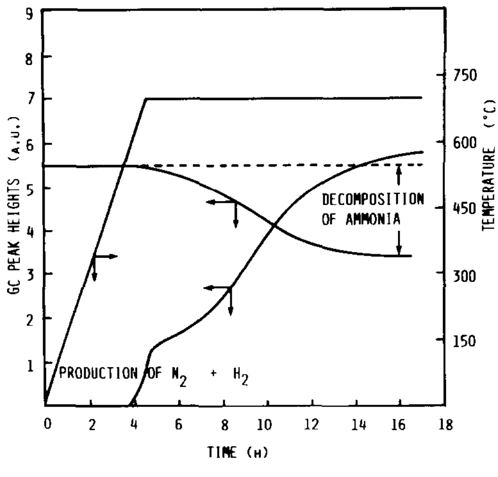

FIG. 1. Evolution of ammonia decomposition versus time during the TiO_2 nitridation.

TABLE I

EFFECT OF SPACE VELOCITY ON FINAL PRODUCT OF TiO_2/NH_3 REACTION

Reference sample	MSV[a] (hr^{-1})	S_{BET} ($m^2\ g^{-1}$)	Phase present[b]	d_{XRD}[c] (nm)	%Nitridation
12NT	70	45	TiN_xO_y	19	70.8
13NT	120	50	TiN_xO_y	20	75.4
14NT	170	52	TiN_xO_y	19	77.4
6NT	220	54	TiN_xO_y	18	74.7

Note. Operating conditions: TiO_2(P25, Degussa) loading, 0.2 g; gas composition in volume, $NH_3/He = 0.48$; heating rate, 50 K/hr; temperature of isothermal treatment, 973 K, duration: 7.5 hr.

[a] Molar space velocity: ratio of molar flow rate of gas to moles of solid precursor.

[b] Detected by XRD.

[c] Crystallite size obtained from (200) X-ray diffraction line broadening analysis.

sults are summarized in Tables I to IV. The effect on nitridation of the low content of rhodium initially mixed with titania was also examined and is reported in Table V.

3.2. Characterization

TEM micrographs of the starting and final materials and electron diffraction pattern of the final solid product are given in Fig. 2.

It is difficult to discern much detail about the texture, which appears very similar to that of the titania precursor. The electron diffraction pattern, which shows rings rather than distinct spots, is indicative of the polycrystalline nature of the sample. The *d*-spacings determined from these rings are characteristic of a fcc lattice and close to those of δ-TiN (*23*, *24*). No other phase was detected.

The XRD analysis at various stages of the synthesis did not show any evidence for the formation of a nitride lower than TiN or of any intermediate oxide between TiO_2 and TiO as was proposed by Kamiya *et al.* (*14*); only the pattern of a fcc phase similar to TiO appeared during the reaction. Above 70% nitridation, the X-ray diffraction data showed the presence of only one fcc phase; its lattice parameter increased with the nitrogen content, from a value close to that of fcc TiO, to a value approaching the parame-

TABLE II

EFFECT OF HEATING RATE ON FINAL PRODUCT OF TiO_2/NH_3 REACTION

Reference sample	Heating rate (K hr^{-1})	S_{BET} ($m^2\ g^{-1}$)	Phase present	d_{XRD} (nm)	%Nitridation
6NT	50	54	TiN_xO_y	18	74.7
15NT	150	55	TiN_xO_y	18	73.1
16NT	205	53	TiN_xO_y	19	73.8

Note. Operating conditions: molar space velocity, 200 hr^{-1}. Other conditions are identical to those reported in footnote *c* to Table I.

TABLE III

EFFECT OF THE TEMPERATURE OF ISOTHERMAL TREATMENT ON THE FINAL PRODUCT OF THE TiO_2/NH_3 REACTION

Reference sample	T_{isoth} (K)	S_{BET} $(m^2\ g^{-1})$	Phase(s) present	d_{XRD} (nm)	%Nitridation
1NT	843	46	Anatase, rutile		8.4
2NT	893	47	Anatase, rutile, TiN_xO_y	11	44.0
3NT	908	48	Anatase, rutile, TiN_xO_y	13	53.1
4NT	933	56	Rutile, TiN_xO_y	16	61.9
5NT	958	58	TiN_xO_y	17	72.4
6NT	973	54	TiN_xO_y	18	74.7
7NT	1013	48	TiN_xO_y	20	80.8
8NT	1058	44	TiN_xO_y	21	85.0
9NT	1093	37	TiN_xO_y	22	88.2
10NT	1118	32	TiN_xO_y	23	90.4

Note. Operating conditions: molar space velocity, 200 hr^{-1}. Other conditions are identical to those reported in footnote *c* to Table I.

TABLE IV

EFFECT OF DURATION OF ISOTHERMAL TREATMENT (908 K) ON FINAL PRODUCT OF TiO_2/NH_3

Reference sample	Duration (hr)	S_{BET} $(m^2\ g^{-1})$	Phase(s) present	d_{XRD} (nm)	%Nitridation
3NT	7.5	48	Anatase, rutile TiN_xO_y	13	53.1
11NT	30	61	TiN_xO_y	16	72.7

Note. Operating conditions: molar space velocity, 200 hr^{-1}. Other conditions are identical to those reported in footnote *c* to Table I.

TABLE V

EFFECT UPON TiO_2 NITRIDATION OF TEXTURE AND/OR LOW CONTENTS OF METAL MIXED WITH TITANIA

	Before nitridation			After nitridation		
Precursor	Pretreatment	S_{BET} $(m^2\ g^{-1})$	Phase(s) present	%Nitridation	S_{BET} $(m^2\ g^{-1})$	Phase(s) present
TiO_2(P25)		46	Anatase, rutile	72.4	58	TiN_xO_y
TiO_2 (aerogels)[a]	O[b]	60	Anatase	76.9	62	TiN_xO_y
TiO_2 (aerogels)[c]	O	59	Anatase	52.9	46	Anatase, TiN_xO_y
2% Rh/TiO_2	O	113	Anatase	70.3	87	TiN_xO_y, Rh

Note. Operating conditions of nitridation: molar space velocity, 200 hr^{-1}. Temperature of isothermal treatment: 958 K. Other conditions are identical to those reported in footnote *c* to Table I.

[a] Aerogel prepared from 30 wt% of titanium tetrabutylate dissolved in butanol.

[b] Samples pretreated under flowing oxygen at 573 K for 2 hr.

[c] Aerogel prepared from 50 wt% titanium tetrabutylate dissolved in butanol.

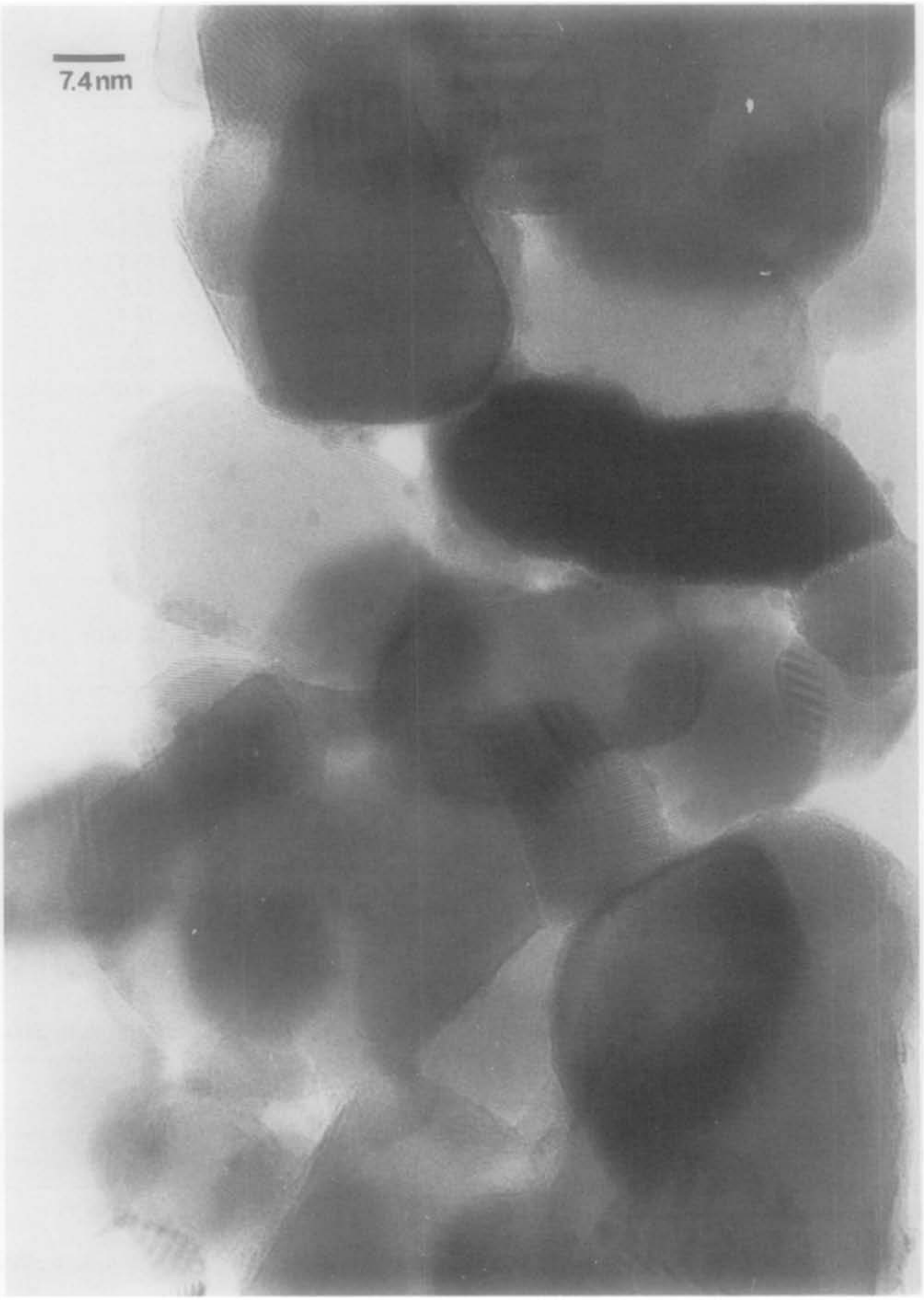

FIG. 2. (a) Transmission electron micrograph of the starting material (TiO_2, P25 Degussa). (b) Transmission electron micrograph and electron diffraction pattern of the final product of the TiO_2/NH_3 reaction.

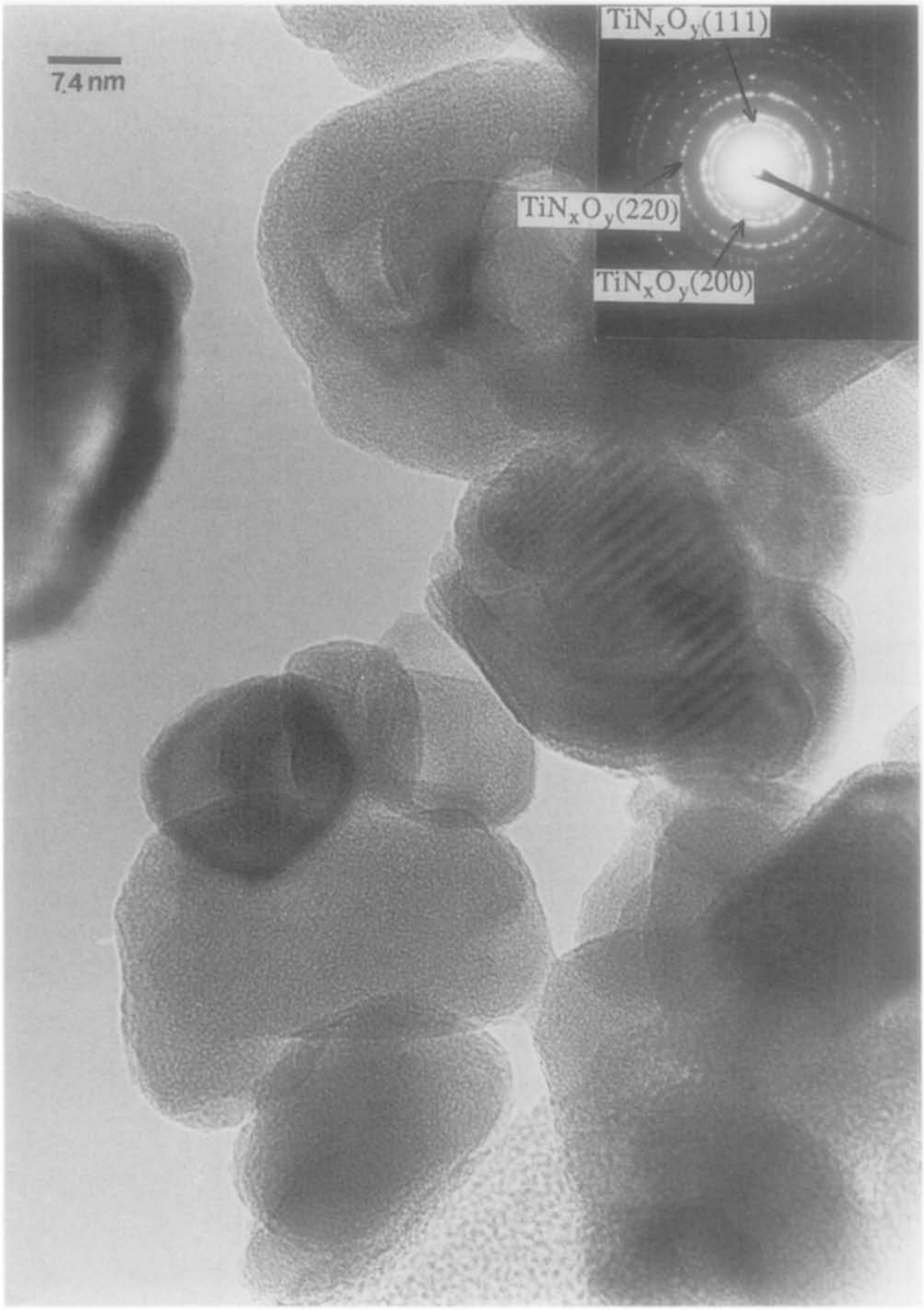

FIG. 2—*Continued*

TABLE VI

EVOLUTION OF XRD PATTERN OF THE FINAL PRODUCT OF TiO_2/NH_3 REACTION VS EXTENT OF NITRIDATION

Sample	$d_{(111)}$ (Å)	I/I°	$d_{(200)}$ (Å)	I/I°	$d_{(220)}$ (Å)	I/I°	a_0(Å)	%Nitridation
$TiO_{(8\text{-}117)}$[a]	2.407	45	2.085	100	1.475	50	4.177	—
3NT	2.4154	45	2.089	100	1.4778	56	4.1842(7)	53.1
4NT	2.4173	49	2.0909	100	1.4790	54	4.1828(6)	63.9
5NT	2.4188	44	2.0933	100	1.4801	49	4.1885(5)	72.4
6NT	2.4200	47	2.0943	100	1.4813	46	4.1902(13)	74.7
7NT	2.4246	51	2.0984	100	1.4836	45	4.1998(4)	80.8
8NT	2.4282	54	2.1022	100	1.4866	43	4.2045(23)	85.0
9NT	2.4332	58	2.1070	100	1.4901	44	4.2179(5)	88.2
17NT	2.4374	63	2.1099	100	1.4922	39	4.2216(6)	91.8
18NT	2.4400	70	2.1127	100	1.4942	38	4.2337(14)	91.9
TiN (38-1420)[a]	2.4492	72	2.1207	100	1.4997	45	4.24173(12)	—

[a] Ref.: X-ray data from JCPDS files.

ter of fcc δ-TiN. In the same time, the relative intensities of the diffraction lines shifted from those characteristic of TiO to those characteristic of δ-TiN (Table VI).

Figure 3 displays a nitrogen adsorption–desorption isotherm obtained for a final product of the TiO_2/NH_3 reaction. The curve shows some features of a type IV isotherm with a narrow hysteresis loop. The pore size distribution is centered on the 15–17 nm range.

Table VII reports elemental analysis for some final single-phase products.

4. Discussion

The evolution of ammonia decomposition versus time provides an indirect indication

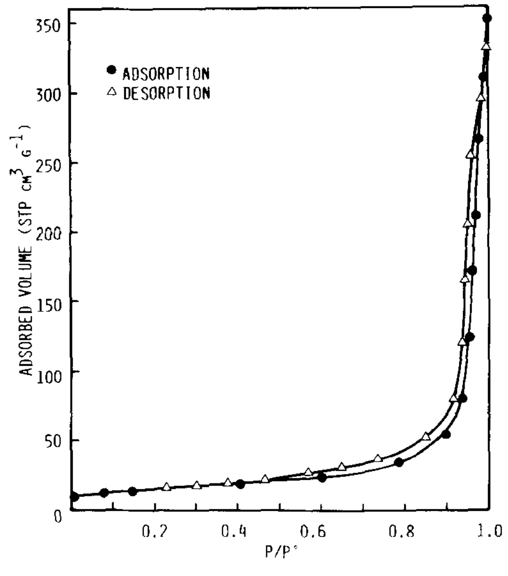

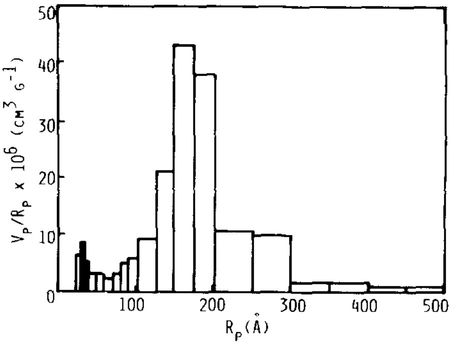

FIG. 3. (a) Nitrogen sorption–desorption isotherm at 77 K for sample 11NT. (b) Pore size distribution histogram.

TABLE VII

ELEMENTAL ANALYSIS OF FINAL PRODUCT OF TiO_2/NH_3 REACTION

Reference sample	%Nitridation	N wt%	O wt%	Ti wt%	Total	Composition[a]
5NT	72.4	16.39	14.73	67.73	98.88	$TiN_{0.83}O_{0.70}$
7NT	80.8	18.27	11.16	70.94	100.37	$TiN_{0.88}O_{0.45}$
9NT	88.2	19.96	7.28	73.14	100.38	$TiN_{0.93}O_{0.28}$
17NT	91.8	20.76	4.31	73.98	99.05	$TiN_{0.92}O_{0.21}$
18NT	91.9	20.79	3.26	77.38	101.43	$TiN_{0.92}O_{0.07}$

[a] Calculated assuming that O wt% = 100 − N wt% − Ti wt%.

on the rate of titania nitridation: this decomposition, by comparison with the thermal behavior of ammonia, appears to be catalyzed by the solid products of the reaction. The measurement of water production would be a more convenient method to follow the nitridation. However, under the actual experimental conditions of synthesis, the rate of reaction was too small so that the water gas-phase concentration was too low to permit a quantitative chromatographic analysis. As a consequence, the extent of nitridation was mainly followed by XRD and elemental analysis of the solid products.

The results show that the heating rate preceding the isothermal treatment had no effect on the composition and on the surface area of the final product. This is consistent with the fact that the rate of nitridation was very slow.

Temperature and duration of isothermal treatment were the effective parameters of the synthesis. Figure 4 shows the evolutions of the surface area and of the degree of nitridation of the final products versus the temperature of the isothermal treatment.

It can be seen that the specific surface area of the products goes through a maximum at about 960 K. The decrease in surface area for samples obtained at higher temperatures can be attributed to hydrothermal sintering, since water was formed during the nitridation; increasing the temperature increased the rate of water production, thereby accelerating the rate of sintering. This explanation is supported by the experimental fact that the surface area of the product decreased with decreasing of the space velocity (Table I) without any significant change in the degree of nitridation.

The stoichiometry of the final product could be estimated when the degree of nitridation reached 70% assuming that only one phase was present. This assumption is suggested by the following considerations:

(i) The XRD and electron diffraction pat-

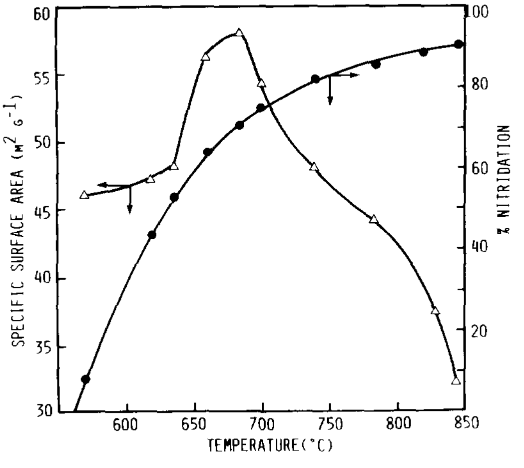

FIG. 4. Specific surface area development and extent of nitridation of the final product of TiO_2/NH_3 reaction as a function of the temperature of isothermal treatment.

terns showed the presence of only one fcc compound.

(ii) The oxygen content of elemental analysis could not be attributed to unreacted TiO_2; otherwise this oxide would have had to be present in amounts (37 to 5 wt%) sufficient to produce an easily detectable diffraction pattern. The formula of the nitride would then lie in the range between $TiN_{1.3}$ and $TiN_{0.9}$, the nitrogen-rich nitride corresponding to the lowest extent of nitridation; this is unexpected. Analogous inconsistent conclusions are reached if the presence of a mixture of both TiO and TiN_x is assumed.

(iii) The evolution of the fcc lattice parameter was clearly correlated to the nitrogen and oxygen contents (Fig. 5).

(iv) The values of this parameter were systematically lower than those reported for the nonstoichiometric mononitride.

For these reasons the fcc phase was considered as a nonstoichiometric oxynitride of general formula TiN_xO_y which tends toward δ-TiN when the nitrogen content rises. This compound is assumed to have a structure similar to that of a disordered TiO phase which is known to have a wide homogeneity range from $TiO_{0.9}$ to $TiO_{1.25}$ at temperatures below about 990°C (*25, 26*).

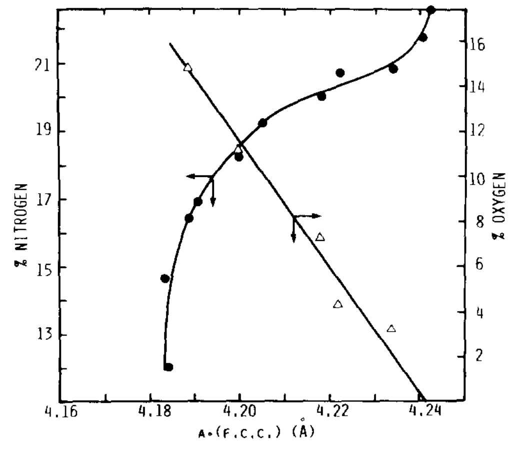

FIG. 5. Evolution of the fcc titanium oxynitride lattice parameter with nitrogen and oxygen contents.

However, this oxynitride differed from that reported by previous workers (*10, 11*) because it has a different lattice parameter; it cannot be considered as a solid solution between TiO and TiN because the elemental analysis data were not compatible with such an assumption. Furthermore, this compound underwent a decomposition at high temperature: when annealed at 1350 K for 24 hr in a sealed evacuated silica tube and rapidly quenched in water, the oxynitride exhibited a two-phase X-ray diffraction pattern corresponding to a mixture of δ-TiN_x and Ti_5O_9 in various amounts according to the degree of nitridation. The x stoichiometry of the δ-nitride phase was evaluated using the lattice parameter–nitrogen content relation determined by Nagakura *et al.* (*24*), to lie between 0.9 to 1.

Thus XRD and elemental analysis data showed that over the temperature range from 890 to 1120 K, the reaction of TiO_2 with ammonia proceeded through the following pathway,

$$TiO_2 \rightarrow TiO \rightarrow TiN_xO_y.$$

In the first step, titania was reduced to a nonstoichiometric TiO, by the atomic hydrogen produced during the ammonia dissociation. Then the process of coreduction/nitridation can be viewed as a kinetic competition between the rates of oxygen removal and nitrogen diffusion.

The oxynitride obtained was not very mesoporous, as is indicated by electron microscopy. The narrow hysteresis loop occuring at $P/P^\circ > 0.9$ could mainly arise from interparticle condensation of nitrogen. The specific surface area of oxynitride was not directly correlated to the specific surface area of the starting material (Table V). Thus, the nitridation of aerogels produced oxynitrides exhibiting specific surface areas lower than those of the starting material; commercial titania yielded oxynitrides with higher specific surface areas. These results show that the thermal stability of the texture of the aerogels was unsuitable for the nitridation, owing to an earlier thermal sintering. However, in the case of a rhodium–titania aerogel, the presence of metal seemed to restrict the effect of the thermal sintering by producing an oxynitride with a specific surface area of 87 $m^2 g^{-1}$.

5. Conclusion

Titania reacted with ammonia between 890 and 1120 K to produce a titanium oxynitride. The composition and specific surface area of this compound depends not only on the temperature and duration of nitridation but also on the texture of titania. In addition, the gas flow rate was a factor influencing the final surface area of the oxynitride. Optimized operating conditions yielded specific surface areas ranging from 58 to 87 $m^2 g^{-1}$ depending on the starting material.

Titanium oxynitride obtained from titania is stable over a large domain of homogeneity; it crystallized in a face-centered cubic lattice. The evolution of the lattice parameter with nitrogen and oxygen contents has been described.

Acknowledgment

The authors acknowledge Professor S. J. Teichner for his assistance in preparing titania aerogels.

References

1. R. B. Levy and M. Boudart, *Science* **181,** 547 (1973).
2. J. M. Muller and F. G. Gault, *Bull. Soc. Chim. Fr.* **2,** 416 (1970).
3. M. Boudart, S. T. Oyama, and L. Leclerc *in* "Proceedings, 7th International Congress on Catalysis, Tokyo, 1980" p. 578, Elsevier, Amsterdam (1981).
4. L. Leclerc, M. Provost, H. Pastor, and G. Leclercq, *J. Catal.* **117,** 384 (1989).
5. M. J. Ledoux, C. Pham-Huu, S. Marin, M. Weibel, and J. Guille, *C.R. Acad. Sci. Ser. 2* **310,** 707 (1990).
6. J. C. Schlatter, S. T. Oyama, J. E. Metcalfe, and J. M. Lambert, *Ind. Eng. Chem. Res.* **27**(9), 1648 (1988).
7. H. C. Jaggers, N. F. Michaels, and M. A. Stacy, *Chem. Mater.* **2,** 150 (1990).
8. S. G. Ranhotra, G. W. Haddix, A. T. Bell, and J. A. Reimer, *J. Catal.* **108,** 24 (1987).
9. G. D. Bogomolov, V. D. Lyubimov, G. P. Shveikin, and S. I. Alyamovskii, *Izv. Akad. Nauk. SSSR Neorg. Mater.* **6,** 1961 (1970).
10. O. Schmitz-Dumont and K. Steinberg, *Naturwissenschaften* **41,** 117 (1954).
11. S. V. Gurov, V. N. Troitskii, V. I. Torbov, and V. V. Kireiko, *Izv. Akad. Nauk. SSSR Neorg. Mater.* **18**(10), 1733 (1982).
12. Y. Motohiko, M. Susumu, *Jpn Kokai Tokkyo Koho JP* **85**-200862 (1985).
13. G. A. Meerson and E. M. Rakitskaya, *Izv. Akad. Nauk. SSSR Neorg. Mater.* **1**(1), 80 (1965).
14. K. Kamiya, T. Yoko, and M. Bessho, *J. Mater. Sci.* **22,** 937 (1987).
15. L. Volpe and M. Boudart, *J. Solid State Chem.* **59,** 332 (1985).
16. S. T. Oyama, J. C. Schlatter, J. E. Metcalfe, and J. M. Lambert, *Ind. Eng. Chem. Res.* **27**(9), 1639 (1988).
17. M. A. Vicarini, G. A. Nicolaon, and S. J. Teichner, *Bull. Soc. Chim. Fr.* **5,** 1651 (1970).
18. S. J. Teichner, G. A. Nicolaon, M. A. Vicarini, and Garde G. E. E., *Adv. Colloid Interf. Sci.* **5,** 245 (1976).
19. D. E. Williams, LCR-2, A Fortran Lattice Constant Refinement Program, USAEC Reports IS-1052 (1964).
20. P. Scherrer, *Göttinger Nachrichten* **2,** 98 (1918).
21. S. Brunauer, P. H. Emmett, and E. Teller, *J. Amer. Chem. Soc.* **60,** 309 (1938).
22. E. P. Barrett, L. G. Joyner, and P. P. Hallenda, *J. Amer. Chem. Soc.* **73,** 377 (1951).
23. P. Ehrlich, *Z. Anorg. Chem.* **259,** 1 (1949).
24. S. Nagakura, T. Kusunoki, F. Kakimoto, and Y. Hirotsu, *J. Appl. Crystallogr.* **8,** 65 (1975).
25. P. Ehrlich, *Z. Anorg. Allg. Chem.* **247,** 53 (1941).
26. S. Anderson, B. Collen, U. Kuylenstierna, and A. Magnéli, *Acta. Chem. Scand.* **11,** 1641 (1957).